PHYSICAL REVIEW B VOLUME 47, NUMBER 7 15 FEBRUARY 1993-I

Secondary-electron production pathways determined by coincidence electron spectroscopy

M. R. Scheinfein
Department of Physics and Astronomy, Center for Solid State Science, Arizona State University, Tempe, Arizona 85287-1504

Jeff Drucker and J. K. Weiss
Center for Solid State Science, Arizona State University, Tempe, Arizona 85287-1504

(Received 19 November 1992)

The production of secondary electrons by fast (100 keV) electrons is investigated by analyzing the time coincidence between inelastically scattered incident electrons and energy-filtered secondary electrons. Thin conducting and semiconducting films show differences in both the coincidence and generation spectra at energies near the bulk-plasmon excitation, suggesting that plasmon decay does not play a central role in the production of secondary electrons in Si. At primary energy losses greater than 35 eV, the secondary-electron production rate is proportional to the energy deposited by the incident electrons.

Structural determination of surfaces, overlayers, and monolayer thin films often utilizes the secondary-electron (SE) signal produced by a focused probe of fast electrons, e.g., surface steps Si(111),[1] Si(100),[2] GaAs(110),[3] Cu(100),[4] NiO, MgO, and Pt.[5] SE production by focused, fast electron beams is a multistage process which includes *excitation* of target electrons by the energetic incident beam, subsequent decay yielding hot SE, *transport* to the surface, and *transmission* over the surface potential barrier.[6] Although the Bethe theory for fast electron inelastic scattering by thin foils has been well understood for over 50 years,[7] detailed theoretical treatments of SE production and transport[6] have yet to be experimentally verified. The role of plasmon decay as a channel for SE production[8] in free-electron metals has received considerable theoretical attention, but remains controversial and awaits experimental characterization.[9]

The multistage model for SE production[6] is poorly characterized, partly due to the experimental difficulty of separating the generation, transport, and transmission processes. The SE generation pathway can be studied by correlating SE of a given energy produced by an initial inelastic excitation using time coincidence detection.[10–12] This technique can determine the role of plasmon decay,[8,9] for example, in the production of SE. The coincidence data presented here suggest that the decay of single-particle-like excitations, rather than plasmons, is the fundamental production channel for SE generated from valence excitations in thin Si films, that each correlated primary energy loss creates a single secondary electron, and that SE generation at energy losses exceeding 35 eV is proportional to the energy deposited by the incident beam.[6]

The experiments were performed in a Vacuum Generators HB501-S UHV scanning transmission electron microscope[13] (STEM) equipped with an electron energy-loss spectrometer (EELS). Surface microanalysis using SE or Auger electron (AE) spectroscopy is performed within the magnetic field of the objective lens using the parallelizer principle.[13,14] The collection efficiency is 100% at SE energies, and degrades to 40% at intermediate AE energies (300–400 eV).

EELS electrons are detected by a single-crystal Ce-doped yttrium-aluminum-garnet (YAG) scintillator while the SE channel employs a channeltron electron multiplier. Time correlation spectra (TCS) are formed by starting the timing electronics with EELS pulses, and using the delayed SE pulses to gate the stop. A time correlation spectrum is acquired at each EEL energy, and the true and false coincidence signals, which are integrals under are TCS peak and background,[15] are extracted and stored. Timing resolution in our system is limited by the fluorescent decay times of the Ce:YAG scintillator which is between 80 and 100 ns. Coincidence spectra acquired at high starting and/or stopping count rates are dead time corrected[15] and verified by analyzing the false coincidence spectrum, the EELS spectrum, and the secondary count rate.[15]

SE production in amorphous (glassy) carbon films has been investigated by Voreades,[10] Mullejans,[11] and Pijper and Kruit.[12] Figure 1 shows our results for SE production in thin (7.5–10 nm) amorphous C films: the valence excitation (0–40 eV) EELS spectrum and the coincidence spectra between EELS electrons and energy-filtered SE [1-eV energy window, Fig. 1(a)] and the SE generation probability [Fig. 1(b)]; all are plotted as a function of primary energy loss. The SE generation probability spectrum is defined as the ratio between the coincidence and EELS spectra,[10–12] and is a measure of SE generation efficiency in a particular inelastic channel. Coincidence spectra onset energies occur at the SE kinetic energy (E_K) plus the work function, $E_K+\phi_W$ ($\phi_W=4.6\pm0.3$ eV) and are a linear function of the measured SE kinetic energy. The peak in each spectrum moves towards higher energy as the SE energy increases.

The coincidence spectra, and the false coincidence spectra not shown, can be integrated over all excitation energies and summed to determine a total SE generation rate. The ratios of the generation rates at given SE energies to the total generation rate for SE of all energies agrees to within 5% with the ratios of the count rates at the same SE energies to the total SE count rate. The total SE production rates predicted by the integrals over the total coincidence spectrum are within 7% of the

 ©1993 The American Physical Society

RAPID COMMUNICATIONS

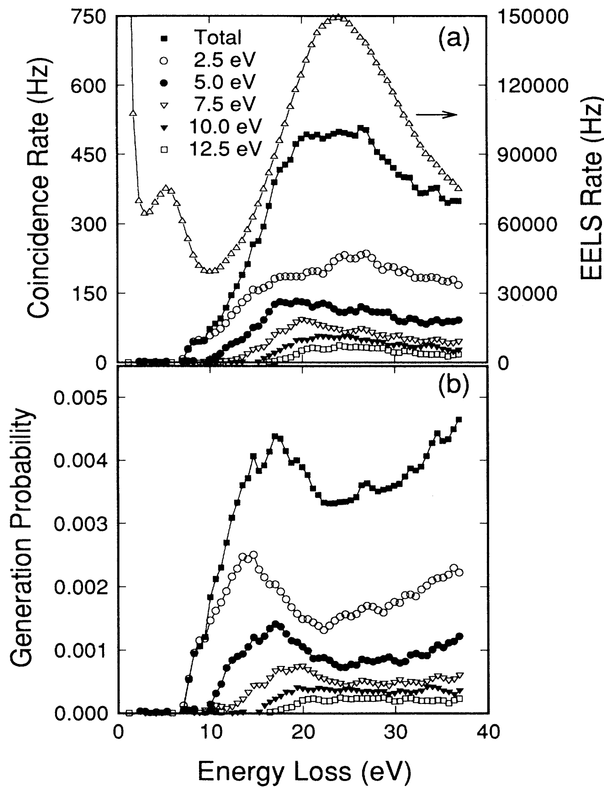

FIG. 1. (a) Transmission valence EELS and coincidence spectra (CNC) between EELS and energy-selected SE (count rate/energy channel) and (b) generation probability spectra, defined as CNC/EELS, for 100-keV electrons incident on a 7.5–10-nm-thick amorphous carbon film as a function of the energy lost by the incident beam. Total SE count rates were 44.8, 22.5, 13.3, 8.7, and 3.3 kHz for 2.5, 5.0, 7.5, 10.0, and 12.5 eV SE, respectively.

current measured at the electrostatic analyzer output. If multiple SE production were an efficient process, then this current meter would record more events than the integral over all coincidence spectra. These data suggest that primary excitations produced by 100-keV incident electrons decay and produce at most a single SE in thin amorphous carbon films, a conclusion qualitatively reached by Mullejans.[11]

The generation probability spectra show pronounced peaks between 15 and 20 eV, with a monotonic increase at excitation energies above 25 eV. Voreades[10] found that the coincidence rate was nearly constant as a function of film thickness, for films thicker than the escape depth for low-energy electrons (typically $t_{\text{escape}}=1.0$–3.0 nm for metals and semiconductors[16]) and thinner than the mean free path for inelastic scattering of the high-energy primary beam ($t_{\text{inelastic}}$ is approximately 50–75 nm for 100-keV electrons in C). Films with $t_{\text{escape}} < t < t_{\text{inelastic}}$ are thick enough to produce the escape-depth limited number of SE, while few SE can be produced by multiply scattered primary electrons. Our data are representative of films in this thickness range. Generation curves for thicker films show an overall decrease in magnitude. This is attributed to increased inelastic scattering for thicker films, while the SE collection is limited by the escape depth for production in proximity to the surface.

EELS, coincidence, and generation probability spectra for p-type ($n_h=10^{15}$ cm^{-3}) Si⟨111⟩ are shown in Fig. 2. The plasmon excitation at 17.7 eV is the dominant feature in the EELS spectrum [Fig. 2(a)]. The excitation energy of the planar surface plasmon[17] [$\omega_s=\omega_p/(1+\epsilon_s)^{1/2}$, where ϵ_s is the real part of the dielectric constant for the medium adjacent to the surface] is a measure of the surface cleanliness. The Si coincidence [Fig. 2(a)] and generation [Fig. 2(b)] spectra are each shifted by 2 Hz (0.001) for visibility. The work function extracted from the data is $\phi_W=4.5\pm0.3$ eV. As for amorphous C, the onset of coincidence shifts towards higher energy linearly with secondary-electron energy.

The role of plasmon decay in SE production remains controversial. These excitations have large cross sections and the accompanying surface plasmons[17] are localized within a SE escape depth of the surface. A number of authors have suggested that plasmons may be a major production pathway for SE in metals[6,8,14] while Massignon *et al.*,[9] in direct contradiction to theoretical predictions, suggested that plasmons were not responsible for SE pro-

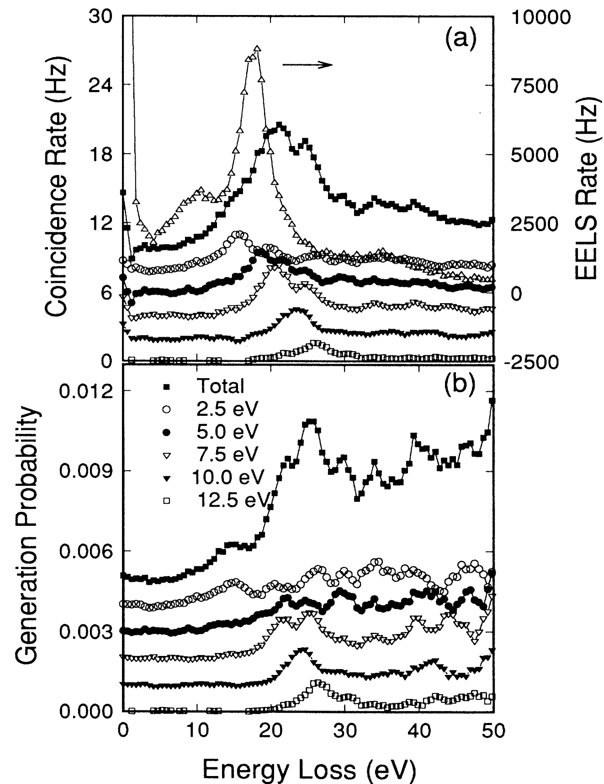

FIG. 2. (a) Transmission valence EELS and CNC between EELS and energy-selected SE (count rate/energy channel) and (b) generation probability spectra, for 100-keV electrons incident on a thin p-type (10^{15} cm^{-3}) Si⟨111⟩ as a function of the energy lost by the incident beam. Total SE count rates were 1.05, 1.17, 1.12, 0.60, and 0.45 kHz for 2.5, 5.0, 7.5, 10.0, and 12.5 eV SE, respectively.

duction in Al. Our data indicate that SE production may be a direct consequence of plasmon decay in amorphous C films while plasmon decay is not the primary production mechanism in *p*-type Si⟨111⟩.

The peak in the total coincidence rate for C between 20 and 24 eV energy loss in Fig. 1(a), and the peak in the generation rate spectrum [Fig. 1(b)] at 18 eV are both below the bulk-plasmon peak in the EELS spectrum at 24 eV. However, the peak in the 2.5-eV [the peak in the $N(E)$ distribution for SE in C] coincidence spectrum between 26 and 28 eV, lies above the plasmon excitation energy. The peaks in the total SE coincidence and generation probability spectra below the plasmon energy suggests that plasmon decay may be a channel for creating SE in thin, amorphous carbon films. The true peak in the C SE spectrum is at 2.5-eV kinetic energy. The 2.5-eV coincidence spectrum has a peak which clearly lies above the plasmon excitation energy, indicating that a substantial fraction of SE results from the decay of inelastic excitations other than volume plasmons.

Peaks in the total Si coincidence and generation probability spectra, Figs. 2(a) and 2(b), lie between 20 and 25 eV, energies well above the plasmon excitation energy. This result suggests that the dominant production pathway for producing secondaries in Si is not plasmon decay but rather single-electron excitations.[17] This conclusion is supported by results which indicate that SE production is enhanced for high momentum transfer events at any one excitation energy.[18] This observation is consistent with the observation that subnanometer spatial resolution images[1-5] can be obtained with secondary electrons, and that plasmon excitations are not suitably localized unless they are produced by high momentum transfer (low impact parameter) collisions.[19] These are the first observations indicating that SE production in semiconductors is clearly not a consequence of the decay of volume plasmons.

If plasmon decay is not a major contributor to the SE yield in semiconductors, then which inelastic events give rise to SE? The data of Fig. 2 provide evidence that interband valence excitations play a major role. The major peaks in the Si coincidence spectra [Fig. 2(a)] scale with the kinetic energy of the emitted secondary electrons. The peaks in the 7.5-eV SE spectra are at 20.0 and 24 eV. Subtracting the SE kinetic energy and the work function from the peak energies indicates that these events originated 8 and 11.7 V below E_F. There are large densities of states (along **L**) at -7.24 and -10.17 eV (Ref. 20) ($E_F=0$). The correspondence between the peaks in the generation spectra and the large density of states along the incident momentum vector suggests that the decay of ionizations from deep in the valence band play a role for SE production in Si(111).

In the Sternglass theory[21] for secondary-electron production, the secondary yield is proportional to the stopping power of the film.[6,22] Normalized generation probability spectra are shown for valence excitations in amorphous carbon [Fig. 3(a)] and ⟨111⟩Si [Fig. 3(b)]. Normalized generation probability spectra consist of generation rate spectra multiplied by the SE energy and divided by the EELS energy. Least-squares fits indicate that the

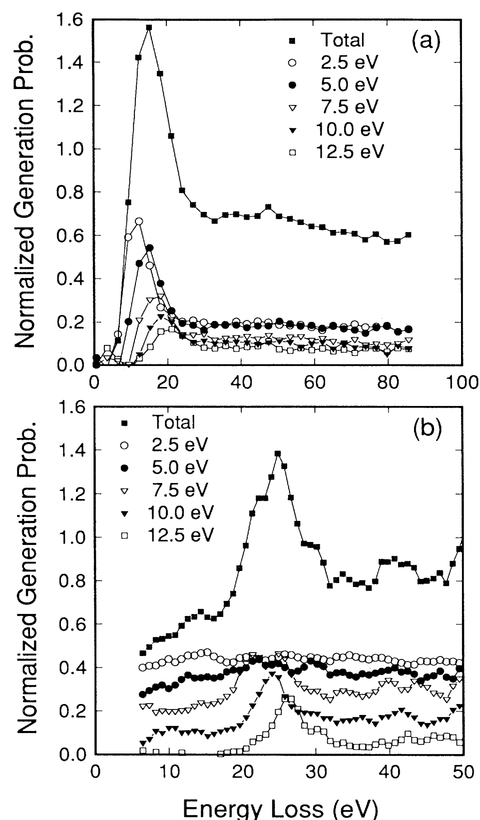

FIG. 3. Normalized generation probability spectra for (a) amorphous carbon and (b) *p*-type ($n_h=10^{15}$ cm^{-3}) Si⟨111⟩.

normalized generation spectra have zero slope to within ±4% for energies between the pronounced peak in the valence excitation region and 100 eV. This suggests that secondary-electron production resulting from energies above the valence-band excitations results from simple energy deposition local to the surface mediated by the escape depth of the SE. The normalized generation probability spectra begin to have negative slope in proximity to, and after the C_K edge.

The largest production cross section for SE production is the valence excitation region. In thin amorphous C, the plasmon decay channel for the production of SE may play an important role. In thin Si, SE production is not primarily a result of bulk-plasmon decay. Our data suggest that the decay of ionizations from deep within the valence band contributes to the SE yield. Normalized generation probability spectra indicate that SE generation is directly proportional to the energy deposited for primary excitations above 35 eV.

We would like to acknowledge A. Higgs for technical support, and Dr. P. Batson, Dr. J. Cowley, Dr. G. Hembree, Dr. M. Isaacson, Dr. J. Liu, Dr. P. Rez, Dr. O. Sankey, and Dr. J. Spence for useful conversations. We acknowledge the NSF-sponsored Center for High Resolution Electron Microscopy at ASU, Grant No. DMR-91-15680.

RAPID COMMUNICATIONS

[1]Y. Homma, M. Tomita, and T. Hayashi, Surf. Sci. **258**, 147 (1991).

[2]J. S. Drucker, M. Krishnamurthy, and G. G. Hembree, Ultramicrosc. **35**, 323 (1991); J. S. Drucker, J. Appl. Phys. **70**, 2806 (1991).

[3]R. H. Milne, Ultramicrosc. **27**, 433 (1989).

[4]A. L. Bleloch, A. Howie, and R. H. Milne, Ultramicrosc. **31**, 99 (1989).

[5]J. Liu and J. M. Cowley, Scanning Microsc. **2**, 65 (1988); Y. Uchida, G. Weinberg, and G. Lempfuhl, Microsc. Res. Technol. **20**, 406 (1992).

[6]D. M. Suszcynsky and J. E. Borovsky, Phys. Rev. A **45**, 6424 (1992); M. Rosler and W. Brauer, Phys. Status Solidi B **104**, 161 (1981); **104**, 575 (1981); **148**, 213 (1988); J. Schou, Scanning Microsc. **2**, 607 (1988); R. Bindi, H. Lateri, and P. Rostaing, *ibid.* **1**, 1475 (1987); V. E. Henrich, Phys. Rev. B **7**, 3512 (1973); R. Willis *et al.*, *ibid.* **9**, 1926 (1974).

[7]H. Bethe, Z. Phys. **76**, 293 (1930); H. Bethe, in *Handbuch der Physik,* edited by H. Geiger and K. Scheel (Springer, Berlin, 1933), Vol. 24/1, p. 273; M. Inokuti, Rev. Mod. Phys. **43**, 297 (1971).

[8]T. E. Everhart and M. S. Chung, J. Appl. Phys. **43**, 3707 (1972); M. S. Chung and T. E. Everhart, Phys. Rev. B **15**, 4699 (1977); J. P. Ganachaud and M. Callier, Surf. Sci. **83**, 498 (1979); **83**, 519 (1979).

[9]D. Massignon, F. Pellerin, J. M. Fontaine, C. LeGressus, and T. Ichinokawa, J. Appl. Phys. **51**, 808 (1980).

[10]D. Voreades, Surf. Sci. **60**, 325 (1976).

[11]H. Mullejans, A. L. Bleloch, A. Howie, and C. McMullan, in IOP Conf. Proc. No. 119 (Institute of Physics and Physical Society, Bristol, 1991), p. 117; H. Mullejans, Ph.D. thesis, University of Cambridge, 1992.

[12]P. Kruit, H. Shuman, and A. P. Somlyo, Ultramicrosc. **13**, 205 (1984); F. J. Pijper and P. Kruit, Phys. Rev. B **44**, 9192 (1991).

[13]G. G. Hembree, P. A. Crozier, J. S. Drucker, M. Krishnamurthy, J. A. Venables, and J. M. Cowley, Ultramicrosc. **31**, 111 (1989).

[14]A. J. Bleeker, Ph.D. thesis, Technische Universiteit Delft, 1991; A. Bleeker and P. Kruit, Nucl. Instrum. Methods A **298**, 269 (1990); P. Kruit and J. A. Venables, Ultramicrosc. **25**, 183 (1988).

[15]T. Akimoto, I. Murai, M. Nakata, and Y. Ogawa, Nucl. Instrum. Methods **184**, 525 (1981); H. Jeremie, Nucl. Instrum. Methods A **244**, 587 (1986); G. F. Knoll, *Radiation Detection and Measurement,* 2nd ed. (Wiley, New York, 1988), Chaps. 4 and 17.

[16]C. J. Powell, Ultramicrosc. **28**, 24 (1988); S. Tanuma, C. J. Powell, and D. R. Penn, J. Vac. Sci. Technol. A **8**, 2213 (1990); J. Electron. Spectrosc. **52**, 285 (1990).

[17]H. Raether, *Plasmons and Intraband Electronic Transitions,* Springer Tracts in Modern Physics Vol. 88 (Springer-Verlag, Berlin, 1982).

[18]Jeff Drucker and M. R. Scheinfein (unpublished).

[19]R. H. Ritchie and A. Howie, Philos. Mag. A **58**, 753 (1988); D. Ugarte, C. Colliex, and P. Trebbia, Phys. Rev. B **45**, 4332 (1992); M. Scheinfein, Scanning Microsc. **1**, 166 (1987).

[20]J. R. Chelikowsky and M. L. Cohen, Phys. Rev. B **14**, 556 (1976).

[21]J. Sternglass, Phys. Rev. **108**, 1 (1957).

[22]M. Cailler and J.-P. Ganachaud, Scanning Microsc. **4**, 57 (1990); **4**, 81 (1990).